Available online at www.sciencedirect.com
SCIENCE DIRECT®
International Journal of Solids and Structures 41 (2004) 6661–6676
INTERNATIONAL JOURNAL OF SOLIDS and STRUCTURES
www.elsevier.com/locate/ijsolstr

Vibration-based construction and extraction of structural damage feature index

Y.J. Yan [a,*], H.N. Hao [b], L.H. Yam [c]

[a] Department of Engineering Mechanics, Institute of Vibration Engineering, Northwestern Polytechnical University, 127 You Yi Road, Xi'an 710072, China
[b] Science School, Xi'an Shi You University, Xi'an 710065, China
[c] Department of Mechanical Engineering, The Hong Kong Polytechnic University, Hung Hom, Kowloon, Hong Kong SAR, China

Received 27 May 2004
Available online 3 July 2004

Abstract

The finite element dynamic model of a honeycomb sandwich plate is presented using different mesh division for the surface plates and the sandwich plate to accurately express the crack damage status of the plate. The experimental measurements of plate natural frequency and dynamic responses are carried out for dynamic model verification. The feasibility of detecting small crack damage according to structural natural frequency and dynamic responses is evaluated. The results show that the energy spectrum of the decomposed wavelet signals of dynamic responses has a higher sensitivity to small crack damage, and more high order modes should be included in the dynamic model for structural damage detection.

Keywords: Crack detection; Natural frequency; Dynamic responses; Wavelet transform; Sandwich plate

1. Introduction

For a long time, great attention has been paid to researches on structural damage detection using structural vibration characteristics. Even for a complex engineering structure in practice, its natural frequencies and dynamic responses at few measured spots can be easily acquired, this fact gives a potential feasibility for the realization of online damage detection and health monitoring of various in-service structures (Farrar et al., 2001). The structural natural frequencies were the earliest used parameters for structural damage detection. Collins et al. (1992) computed the frequency spectra and studied the effects of crack location on longitudinal vibrations of a cantilevered bar with a transverse crack. Nandwana and Maiti (1997) added a rotational spring to a slender beam for crack simulation in

* Corresponding author. Tel.: +86-29-88492895; fax: +86-29-88492216.
E-mail address: hnhao@xsyu.edu.cn (Y.J. Yan).

0020-7683/$ - see front matter © 2004 Elsevier Ltd. All rights reserved.
doi:10.1016/j.ijsolstr.2004.05.069

order to check the feasibility of detecting crack location based on the measurement of natural frequencies, and pointed out that when the internal crack depth is more than 20% of the section depth, the detection performance was satisfactory. Ramamurti and Neogy (1998) considered the feasibility of using natural frequency as a criterion for damage detection, and concluded that natural frequency does not appear to be an appropriate criterion for integrity analysis in a simplified model. Salawu (1997) reviewed plentiful literatures about structural damage detection using the natural frequency and discussed the possible limit factors for successful application of vibration monitoring to damage detection and structural assessment. Many researches on structural damage detection using the online measured structural vibration responses have also been carried out (Zou et al., 2000). Hou et al. (2000) used the characteristics of the wavelet transformation of simulated vibration response signals generated from a simple structural model subjected to a harmonic excitation. They showed a great promise of the wavelet approach for damage detection and structural health monitoring. Zhang et al. (1999) adopted vibration measurements to detect structural damage using Transmittance Function Monitoring, and the parameters used for damage detection were computed from different types of measured structural responses.

Although the two above-mentioned methods are simple and easy to execute, there are still many problems in the realization of damage detection for practical engineering structures. Because a small quantity of structural information is adopted, it is difficult to detect a practical complex structural damage status, such as determination of damage location, damage category and extent as well as some small structural damage. Therefore, some researchers adopted more structural information in structural damage detection, for example, mode shapes (Kosmatka and Ricles, 1999; Hu et al., 2001), modal strain energy (Doebling et al., 1997; Chen et al., 2000), etc. However, these methods require a large amount of measured data or numerical simulation using an accurate structural dynamic model. This is not advantageous for online damage detection of an in-service structure.

Identifying damage status from global dynamic behaviors of a structure is essentially an inverse problem of structural dynamic analysis. The issues to be solved include identification of structural damage category, extent and location. Because practical engineering problems are generally very complex, structural damage detection using vibration method is always conducted in two steps, one is to determine if damage has occurred, the other is to identify the category, extent and location of structural damage. Many researchers have adopted some simple structural model, such as a beam, to study damage detection, but for complex engineering structures some conclusions may not be the same.

Honeycomb sandwich composite plates have been widely applied to aeronautical structures as well as building, automobile and train structures because it possesses many advantages, such as lighter weight, higher stiffness, heat insulation and preservation, and anti-radialization (the structure can resist the radialization from electromagnetic wave or infrared ray when structural material is mixed by some material that can absorb electromagnetic wave or infrared ray). This kind of structural materials are made of very thin aluminum alloy, FRP (fiberglass-reinforced plastics), PVC and CFRBP (ceramic fiber round braided rope), etc. One of its most excellent properties is the lightweight, and its weight is only 10–15% of that of a solid structure with the same material. However, the ability of resisting impact of a honeycomb sandwich plate is very poor, so crack or unglued damage occurs frequently. This will seriously affect the function of the structural components, such as the propeller of a helicopter, aerofoil and sealed-cabin. Obviously, the study of in-service damage detection for honeycomb sandwich structures possesses significant application values.

This paper aims at evaluating feasibility of structural crack damage detection using vibration parameters. A more accurate finite element dynamic model of a honeycomb sandwich plate, which is closer to some practical engineering structures, is established. Its natural vibration traits and response characteristics are checked by experimental measurements. Various possible influences of crack damage status on structural natural frequency and responses are discussed.

2. Dynamic finite element model of a sandwich plate with crack damage

When a crack exists in a honeycomb sandwich plate (as shown in Fig. 1), it can be described using five parameters: depth d, length l, directional angle α and location coordinates x_c and y_c. Assume that only very narrow crack is considered, the crack width can be approximately taken as zero. A crack damage status can be expressed as

$$g = g(x_c, y_c, l, d, \alpha) \tag{1}$$

Crack damage in a sandwich plate will lead to a structural stiffness reduction of the local area as well as the whole structure. Therefore, structures with different location and extent of crack will exhibit different dynamic features. In the finite element model established for this study, the crack parameters including location, length and directional angle are expressed using the nodal coordinates of two adjacent eight nodes quadrangular elements I and II as shown in Fig. 2(a). According to different size and shape of the two elements, various cracks can be simulated.

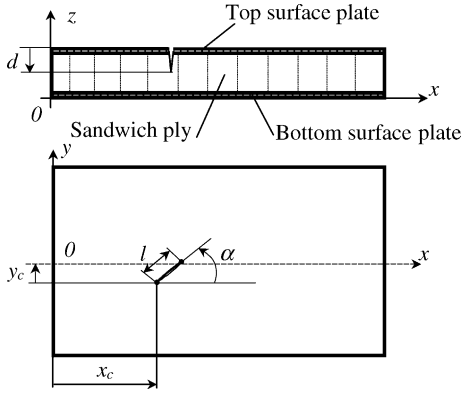

Fig. 1. Crack damage in a honeycomb sandwich plate.

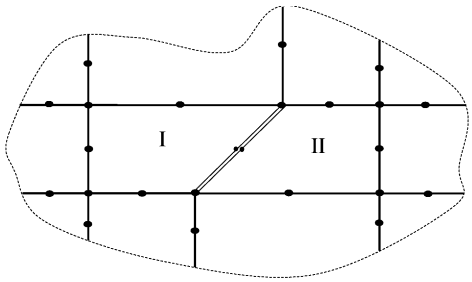

(a) A crack in surface plate

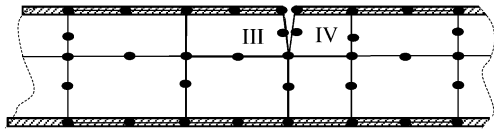

(b) A crack in stiffened plate

Fig. 2. Element division of a honeycomb sandwich plate with crack damage.

Assume that the crack depth reaches the inside of sandwich ply of the plate. In the present study, a kind of sandwich ply made of stiffened plate is studied. In order to deal with the crack depth, the top and bottom plates, and the stiffened plate are independently divided into quadrangular elements as shown in Fig. 2(b), and the different vertical dimension of the two adjacent quadrangular elements III and IV can represent the variation of the crack depth.

Assume that the top and bottom surfaces, and all the stiffened plates are isotropic thin plates and subjected to a small elastic bending distortion. Three types of mid-plane coordinates: $o_t x_t y_t z_t$; $o_b x_b y_b z_b$ and $o_i x_i y_i z_i$, are used respectively for these three parts. Displacements in x-, y- and z-directions can be expressed respectively as

$$\left.\begin{array}{lll} u_t = -z_t\theta_{tx}, & v_t = -z_t\theta_{ty}, & w_t = w_t(x_t, y_t), \\ u_b = -z_b\theta_{bx}, & v_b = -z_b\theta_{by}, & w_b = w_b(x_b, y_b), \\ u_i = -y_i\theta_{ix}, & v_i = v_i(x_i, z_i), & w_i = -y_i\theta_{iz}. \end{array}\right\} \tag{2}$$

At the common nodes of the top and stiffened plates or the bottom and stiffened plates, the continuous conditions of the displacement give $w_t = w_i$, $u_t = u_i$, and $v_t = v_i$ or $w_b = w_i$, $u_b = u_i$ and $v_b = v_i$. Strains in these three parts can be expressed as

$$\{\varepsilon\}_t = \left\{ -z_t\frac{\partial\theta_{tx}}{\partial x_t}, -z_t\frac{\partial\theta_{ty}}{\partial x_t}, -z_t\left(\frac{\partial\theta_{tx}}{\partial x_t} + \frac{\partial\theta_{ty}}{\partial x_t}\right)\right\}^{\mathrm{T}}, \tag{3}$$

$$\{\varepsilon\}_b = \left\{ -z_b\frac{\partial\theta_{bx}}{\partial x_b}, -z_b\frac{\partial\theta_{by}}{\partial x_b}, -z_b\left(\frac{\partial\theta_{bx}}{\partial x_b} + \frac{\partial\theta_{by}}{\partial x_b}\right)\right\}^{\mathrm{T}}, \tag{4}$$

$$\{\varepsilon\}_i = \left\{ -y_i\frac{\partial\theta_{iz}}{\partial z_i}, -y_i\frac{\partial\theta_{ix}}{\partial x_i}, -y_i\left(\frac{\partial\theta_{iz}}{\partial z_i} + \frac{\partial\theta_{ix}}{\partial x_i}\right)\right\}. \tag{5}$$

An arbitrary quadrangular element in a Cartesian coordinate system can be transformed into a rectangular element using a set of the following transform

$$\begin{Bmatrix} x \\ y \end{Bmatrix} = f\begin{Bmatrix} \xi \\ \eta \end{Bmatrix}. \tag{6}$$

Assume that the nodal coordinate of an arbitrary quadrangular element is (x_j, y_j); $j = 1, 2, \ldots, 8$, and the element shape function is $N_j(\xi, \eta)$; $j = 1, 2, \ldots, 8$, then Eq. (6) can be expressed as

$$x = \sum_{j=1}^{8} N_j(\xi, \eta)x_j, \qquad y = \sum_{j=1}^{8} N_j(\xi, \eta)y_j. \tag{7}$$

The displacements in Eq. (2) can be written as

$$w_t = \sum_{j=1}^{8} N_j w_{tj}, \qquad \theta_{tx} = \sum_{j=1}^{8} N_j\theta_{txj}, \qquad \theta_{ty} = \sum_{j=1}^{8} N_j\theta_{tyj}, \tag{8}$$

$$w_b = \sum_{j=1}^{8} N_j w_{bj}, \qquad \theta_{bx} = \sum_{j=1}^{8} N_j\theta_{bxj}, \qquad \theta_{by} = \sum_{j=1}^{8} N_j\theta_{byj}, \tag{9}$$

$$\theta_{iz} = \sum_{j=1}^{8} N_j\theta_{izj}, \qquad \theta_{ix} = \sum_{j=1}^{8} N_j\theta_{ixj}, \qquad v_i = \sum_{j=1}^{8} N_j v_{ij}, \tag{10}$$

where the element shape function $N_j(\xi,\eta)$ is as follows

$$N_j(\xi,\eta) = (1+\xi\xi_j)(1+\eta\eta_j)(\xi\xi_j+\eta\eta_j-1)\xi_j^2\eta_j^2/4 + (1-\xi^2)(1+\eta\eta_j)(1-\xi_j^2)\eta_j^2/2 + (1-\eta^2)(1+\xi\xi_j)(1-\eta_j^2)\xi_j^2/2, \quad j=1,2,\ldots,8. \tag{11}$$

The displacement vector at the jth node for bending deformation of a thin plate can be written as

$$\{\delta_t^j\} = [w_{tj},\theta_{txj},\theta_{tyj}]^{\mathrm{T}}, \qquad \{\delta_b^j\} = [w_{bj},\theta_{bxj},\theta_{byj}]^{\mathrm{T}}, \qquad \{\delta_i^j\} = [\theta_{izj},\theta_{ixj}v_{ij}]^{\mathrm{T}}. \tag{12}$$

For the top plate, using the regular procedures of FEM (Huebner, 2001), one can obtain the equation of motion of an element as follows

$$[M^{\mathrm{e}}]_{24\times24}\{\ddot{\delta}^{\mathrm{e}}\}_{24\times1} + [K^{\mathrm{e}}]_{24\times24}\{\delta^{\mathrm{e}}\}_{24\times1} = \{F^{\mathrm{e}}\}_{24\times1}, \tag{13}$$

where $[M^{\mathrm{e}}]$, $[K^{\mathrm{e}}]$ and $\{F^{\mathrm{e}}\}$ are element mass matrixes, stiffness matrix and nodal force vector, respectively. $\{\ddot{\delta}^{\mathrm{e}}\}$ and $\{\delta^{\mathrm{e}}\}$ are nodal acceleration and displacement vectors, respectively. Hereinto,

$$[M^{\mathrm{e}}]_{24\times24} = \int_{-1}^{1}\int_{-1}^{1}\mathbf{G}^{\mathrm{T}}\mathbf{P}\mathbf{G}|\mathbf{J}|\,\mathrm{d}\xi\,\mathrm{d}\eta, \qquad [K^{\mathrm{e}}]_{24\times24} = \int_{-1}^{1}\int_{-1}^{1}\mathbf{B}^{\mathrm{T}}\mathbf{D}\mathbf{B}|\mathbf{J}|\,\mathrm{d}\xi\,\mathrm{d}\eta, \tag{14}$$

where the Jacobi determinant $|\mathbf{J}|$, elastic matrix $\mathbf{D}$ and mass density matrix $\mathbf{P}$ are as follows:

$$|\mathbf{J}| = \begin{vmatrix} \frac{\partial x}{\partial\xi}, & \frac{\partial y}{\partial\xi} \\ \frac{\partial x}{\partial\eta} & \frac{\partial y}{\partial\eta} \end{vmatrix}, \qquad \mathbf{D} = \frac{Eh^3}{12(1-\mu^2)}\begin{bmatrix} 1 & \mu & 0 \\ \mu & 1 & 0 \\ 0 & 0 & \frac{1-\mu}{2} \end{bmatrix}, \qquad \mathbf{P} = \rho\begin{bmatrix} h & 0 & 0 \\ 0 & \frac{1}{12}h^3 & 0 \\ 0 & 0 & \frac{1}{12}h^3 \end{bmatrix}, \tag{15}$$

where E, μ and ρ are the elastic modulus, Poisson's ratio and mass density of the structural material, respectively, and h is the plate thickness. In Eq. (14), the strain matrix $\mathbf{B}$ and velocity matrix $\mathbf{G}$ are as follows:

$$\left.\begin{aligned} \mathbf{B} &= [(\mathbf{B}_1)_{3\times3},(\mathbf{B}_2)_{3\times3},\ldots,(\mathbf{B}_8)_{3\times3}], \\ \mathbf{G} &= [(\mathbf{G}_1)_{3\times3},(\mathbf{G}_2)_{3\times3},\ldots,(\mathbf{G}_8)_{3\times3}], \end{aligned}\right\} \tag{16}$$

where

$$\mathbf{B}_j = \begin{bmatrix} -\frac{\partial N_j}{\partial x_t} & 0 & 0 \\ 0 & -\frac{\partial N_j}{\partial y_t} & 0 \\ -\frac{\partial N_j}{\partial x_t} & -\frac{\partial N_j}{\partial y_t} & 0 \end{bmatrix}, \qquad \mathbf{G}_j = \begin{bmatrix} -N_j & 0 & 0 \\ 0 & -N_j & 0 \\ 0 & 0 & N_j \end{bmatrix}, \quad j=1,2,\ldots,8. \tag{17}$$

Similar procedures can be used to establish the element equations of motion of the bottom and stiffened plates. Assembling all element equations of motion of the three kinds of plates, one can obtain the following equation of motion of the whole honeycomb sandwich plate without considering damping:

$$\mathbf{M}\ddot{\Delta} + \mathbf{K}\Delta = \mathbf{F}, \tag{18}$$

where $\mathbf{M}$, $\mathbf{K}$ and $\mathbf{F}$ are the global mass matrix, stiffness matrix of the structure and the external force vector, respectively. $\ddot{\Delta}$ and Δ are the global nodal acceleration and displacement vectors, respectively. Assume that the structure has proportional damping as follows:

$$\mathbf{C} = \alpha\mathbf{M} + \beta\mathbf{K}, \tag{19}$$

where $\mathbf{C}$ is the global damping matrix, and α and β are the proportional damping coefficients. To execute modal transform to Eq. (19) using the normalized modal matrix Φ, one can get

$$\Phi^{\mathrm{T}}\mathbf{C}\Phi = \Phi^{\mathrm{T}}(\alpha\mathbf{M}+\beta\mathbf{K})\Phi \Rightarrow 2\zeta_i\omega_i = \alpha + \beta\omega_i^2 \quad (i=1,2,\ldots,n),$$

where ω_i and ζ_i are the ith natural frequency and modal damping ratio, respectively. For arbitrary $i \neq j$, the α and β can be solved using following equation:

$$\left.\begin{aligned}\alpha+\beta\omega_i^2 &= 2\varsigma_i\omega_i,\\ \alpha+\beta\omega_j^2 &= 2\varsigma_j\omega_j,\end{aligned}\right\} \Rightarrow \left.\begin{aligned}\alpha &= 2\varsigma_i\omega_i - 2\omega_i^2(\varsigma_j\omega_j-\varsigma_i\omega_i)/(\omega_j^2-\omega_i^2),\\ \beta &= 2(\varsigma_j\omega_j-\varsigma_i\omega_i)/(\omega_j^2-\omega_i^2).\end{aligned}\right\}$$

Though modal damping ratio ζ_i and ζ_j may have some difference for different modes, they mainly depend on structural material property. Generally, steel $\zeta_i \approx 0.005$, concrete $\zeta_i \approx 0.08$, felt or cork $\zeta_i \approx 0.06$, natural rubber $\zeta_i \approx 0.05$, etc. Supposing that $\varsigma_i \approx \varsigma_j = \varsigma$, one can get the approximate formula as follows

$$\left.\begin{aligned}\alpha &\approx 2\varsigma\omega_i[1-\omega_i/(\omega_i+\omega_j)],\\ \beta &\approx 2\varsigma/(\omega_j+\omega_i).\end{aligned}\right\} \tag{20}$$

Combining Eqs. (18) and (19), the structural equations of motion can be expressed as

$$\mathbf{M}\ddot{\Delta}+\mathbf{C}\dot{\Delta}+\mathbf{K}\Delta=\mathbf{F}. \tag{21}$$

3. Vibration-based structural damage feature index

When some crack occurs in a honeycomb sandwich plate, the plate natural frequency, modal shapes, frequency response functions and dynamic response properties, etc. will vary with the location and extent of the cracks because of the variations of local structural stiffness. In order to emphatically evaluate the influence of crack location and extent on the above-mentioned dynamic characteristics, the situation with only one crack is considered in this paper.

For a honey comb sandwich plate with crack damage status $g = g(a, c, l, d, \alpha)$, if the structural damping is neglected and the external load equals zero, Eq. (21) can be written as

$$\mathbf{M}\ddot{\Delta}+\mathbf{K}(g)\Delta=\mathbf{0}. \tag{22}$$

Solving Eq. (22), one can get its eigenvalue $\omega_i(g)$ and mode vector $\Phi_i(g)$, which vary with crack damage status g, and $i = 1, 2, \ldots, n$, where n is the number of structural mode considered in this study.

Vibration responses at few spots of an in-service structure can be easily measured using the technology of piezoelectric smart structures (Gobin et al., 2000). However, the raw response signal in time domain cannot be used directly to identify structural damage quantitatively. Some representative indexes have to be selected and constructed. Wavelet transform of response signals is one of the available methods. Wavelet analysis of time-varying signal is a kind of localization analysis method in time and frequency domains, and the time and frequency windows can both be changed. This signal processing method has higher frequency and time resolution (Chui, 1997).

A continuous wavelet transform of a function $f(t) \in L^2(R)$ is defined as

$$W_f(a,b)=\frac{1}{\sqrt{|a|}}\int_R f(t)\Psi^*\left(\frac{t-b}{a}\right)\mathrm{d}t, \tag{23}$$

where b is the translation parameter, a is the scale parameter, $f(t)$ is the function (signal) to be transformed, $\Psi^*(t)$ is the transforming function (mother wavelet), W_f is the calculated wavelet coefficients, which can be used to recompose the original function $f(t)$. The re-composition equation can be expressed as

$$f(t)=\frac{1}{C_\Psi}\int_{-\infty}^{+\infty}\int_{-\infty}^{+\infty}\frac{1}{a^2}W_f(a,b)\Psi\left(\frac{t-b}{a}\right)\mathrm{d}a\,\mathrm{d}b, \tag{24}$$

where $C_\Psi = \int_0^{+\infty} \frac{|\widehat{\Psi}(\omega)|^2}{|\omega|} \mathrm{d}\omega < \infty$, and $\widehat{\Psi}(\omega)$ is the Fourier transform of Mother Wavelet $\Psi(t)$. The various forms of mother wavelet $\Psi(t)$ have now been developed.

In practical application for wavelet transforms, especially in order to realize numerical simulation in computer, the continuous wavelet must be changed into discrete form. One of the most usually used discrete wavelet is Dyadic Wavelet (binary wavelet), i.e.

$$\Psi_{j,k}(t) = 2^{-j/2}\Psi(2^{-j}t - k), \quad j,k \in Z. \tag{25}$$

Therefore, the discrete wavelet transforms and re-composing (invert wavelet transform) of a function $f(t)$ can be written as

$$W_{2^j} f(k) = 2^{-j} \int_R f(t)\Psi^*(2^{-j}t - k)\,\mathrm{d}t, \tag{26}$$

$$f(t) = \sum_{j\in Z} \int W_{2^j} f(k)\Psi_{2^j}(2^{-j}t - k)\,\mathrm{d}k, \tag{27}$$

where $W_{2^j} f(k)$ denotes one variable, i.e. the wavelet transform of $f(t)$.

The wavelet package analysis (WPA) is the most useful method of wavelet transform. It can adaptively choose the corresponding frequency bandwidth according to the characteristics of the signal to be analyzed, so that the resolution in frequency and time domains can both be enhanced.

The WPA algorithm is as follows.

Let $g_j^n(t) \in U_j^n$, then $g_j^n(t)$ can be expressed as

$$g_j^n(t) = \sum_l d_l^{j,n} u_n(2^j t - l), \tag{28}$$

where $g_j^n(t)$ is an arbitrary function in sub-space U_j^n. $u_n(2^j t - l)$ is the orthogonal wavelet packet, and $d_l^{j,n}$ is the decomposed wavelet packet coefficient. The WPA decomposed coefficient is calculated by equation as follows

$$\left.\begin{array}{l} d_l^{j,2n} = \sum_k a_{k-2l} d_k^{j+1,n}, \\ d_l^{j,2n+1} = \sum_k b_{k-2l} d_k^{j+1,n}, \end{array}\right\} \tag{29}$$

where a_{k-2l} is the low-pass digital filter and b_{k-2l} is the high-pass digital filter.

The WPA re-composing is to calculate $\{d_l^{j+1,n}\}$ using $\{d_l^{j,2n}\}$ and $\{d_l^{j,2n+1}\}$, and equation as follows

$$d_l^{j+1,n} = \sum_k [h_{l-2k} d_k^{j,2n} + g_{l-2k} d_k^{j,2n+1}], \tag{30}$$

where h_{l-2k} is the low-pass digital filter and h_{l-2k} is the high-pass digital filter.

The theory of wavelet analysis is very profuse, and the interested researcher can refer to references (Mallat, 1999; Strang and Nguyen, 1996).

Energy of dynamic response of cracked structures compared with that of the intact structure in some special frequency bands will exhibit some remarkable difference. This is because the structural damage will suppress or enhance some components of response signal in special frequency bands, i.e., the structural damage can cause energy increase of some response signal components or energy decrease of other response signal components. Therefore, the energy of structural vibration response signals with different frequency components contains ample information of structural damage, and the energy variation of one or several frequency components of the signals can indicate a special status of structural damage.

In order to extract structural damage information from structural response signal, the signal is first decomposed into multiple sub-signals in various frequency bands using WPA. Let $S_{00}(t)$ denote the original signal of structural response, it can be expressed as

$$S_{00}(t) = \sum_{j=1}^{2^{k-1}} S_{kj}(t), \tag{31}$$

where $S_{kj}(t)$ is the sub-signal with orthogonal frequency band and k indicates the layer number of the tree structure of wavelet decomposition.

The energy of these sub-signals can be expressed as

$$U_{kj} = \int |S_{kj}(t)|^2 \, \mathrm{d}t. \tag{32}$$

A non-dimensional index vector can be composed using U_{kj}^0 and $U_{kj}(j = 0, 1, 2, \ldots, 2^{k-1})$, i.e.

$$V_\mathrm{d} = \{\Lambda_1, \Lambda_2, \ldots, \Lambda_{2^{k-1}}\}, \qquad \Lambda_j = 1 - \frac{U_{kj}}{U_{kj}^0}, \qquad j = 1, 2, \ldots, 2^{k-1}, \tag{33}$$

where U_{kj}^0 and U_{kj} are the sub-signal energy of the intact and crack damaged plates, respectively. Λ_j indicates the magnitude variation of the jth order sub-signal energy, it is a measurement of the enhancement or attenuation of the jth order sub-signal energy.

We also find that when different mother wavelet is adopted for decomposition of vibration response of structure with damage, the obtained "the energy index" is quite different. In this study, we have attempted to use several mother wavelets, and found the Daubechies wavelet (db5) has the better effect for indication of structural damage. In numerical simulation, the wavelet analysis toolbox in the MATLAB software is used, so that programme design can be greatly simplified.

4. Numerical simulation and experiment

The structural damage status, such as damaged locations, extents and categories, of a practical engineering structure is related to a large amount of information and data. It is not reasonable to acquire such information only using experiment or numerical simulation. Superfluous experimental work is time consuming and not economical, and numerical simulation without experimental verification is unbelievable. A more scientific way is to use a more accurate structural dynamic model checked by experiment for numerical simulation to acquire a large amount of information and data related to structural damage status.

The specimen of the numerical model is a honeycomb sandwich cracked plate as shown in Fig. 3, and it has length L, width B and thickness h of 295, 98 and 8 mm, respectively. The plate is composed of PVC materials, and its top surface has a thin aluminium raincoat. The plate weight is only 12.67% of a solid structure with the same dimension and material. The PVC material parameters are $E = 3.5$ GPa, $\mu = 0.34$ and $\rho = 1.36$ kg/m^3.

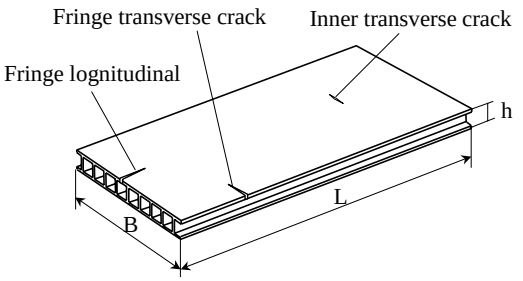

Fig. 3. Specimen of a honeycomb sandwich plate with crack damage.

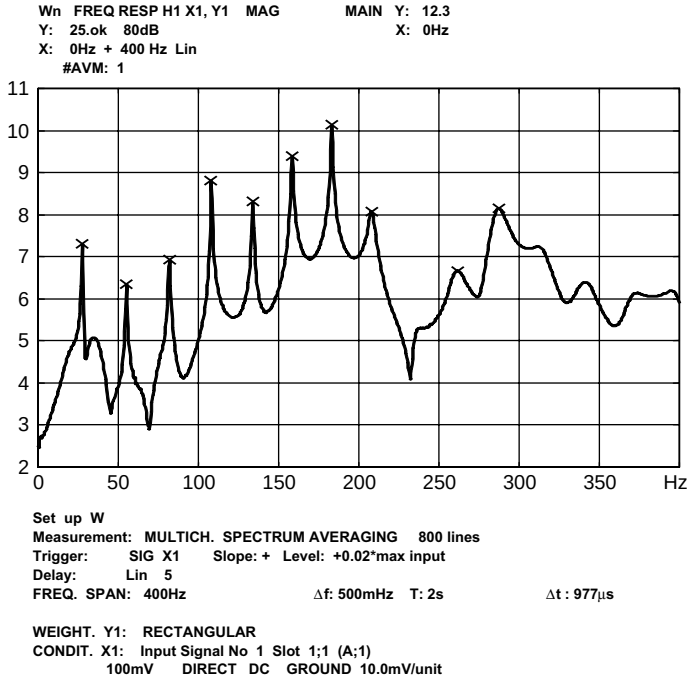

Fig. 4. Experimental frequency–response curve of the specimen.

The natural frequencies of an undamaged specimen of honeycomb sandwich plate are experimentally measured to verify the reliability of the theoretical formula and programs. An experimental frequency response curve is given in Fig. 4. The lowest 10 natural frequencies acquired by experiment and simulation and the percentage errors between the results obtained using these two methods are listed in Table 1, which shows that the errors are below 5%. This is an acceptable numerical precision in engineering problems. The lowest 10 elastic mode shapes acquired by simulation are shown in Fig. 5.

Based on the dynamic model verified by the experiment, the natural frequencies of the honeycomb sandwich plate for various crack damage status are numerically computed. When the crack width is extremely small and negligible, crack length will be the most important factor to affect structural dynamic

Table 1
Natural frequencies of the intact honeycomb sandwich plate obtained by experiment and numerical simulation

Order	Numerical	Experiment	Errors
1	29.711 Hz	28.5 Hz	4.2%
2	50.900 Hz	52.5 Hz	3.0%
3	80.826 Hz	82 Hz	1.4%
4	106.99 Hz	108 Hz	1.0%
5	139.70 Hz	134 Hz	4.2%
6	162.70 Hz	158.5 Hz	2.6%
7	192.16 Hz	184 Hz	4.4%
8	212.43 Hz	208 Hz	2.1%
9	250.42 Hz	261.5 Hz	4.2%
10	277.07 Hz	287.5 Hz	3.6%

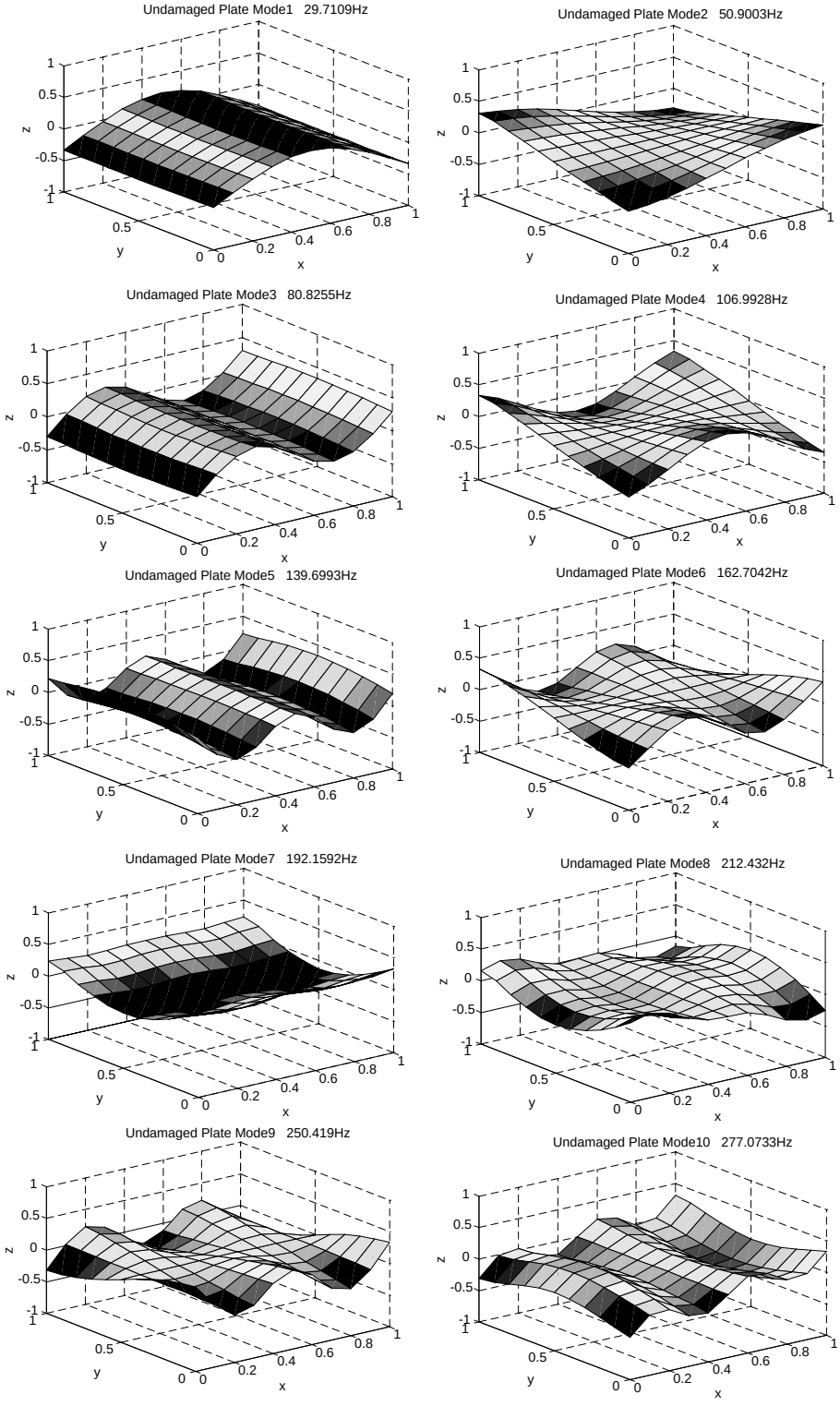

Fig. 5. Elastic mode shapes of a plate with free boundary conditions.

characteristics. Besides, crack directions also have influence on an anisotropic plate, and the crack location in a plate also needs to be studied. First, the plate natural frequencies for damage status of different crack length with longitudinal and transverse cracks (parallel and perpendicular to the stiffened plates, see Fig. 3) are calculated, and they are listed in Table 2.

According to the analysis of data in Table 2, some conclusions can be drawn as follows:

(1) If a crack length is less than 5% of plate length or width, the natural frequencies nearly have no change except for some particular mode, such as the 7th frequency in damage status of longitudinal inner crack, i.e., crack away from the plate edges.
(2) If a crack length is less than 10% of plate length or width, some changes may occur in certain orders of natural frequencies, such as the 6th and 7th frequencies in damage status of longitudinal and transverse inner crack.
(3) If a crack length is longer than 20% of plate length or width, there will be remarkable changes in multiple natural frequencies. However, a practical structure with such large crack may have already failed.
(4) Results show that changes in the natural frequency of a cracked plate do not always appear in the lowest modal frequencies.
(5) For an anisotropic sandwich plate, the sensitivity of natural frequency to transverse crack is lower than that to longitudinal crack.

In order to evaluate the influence of crack location on plate natural frequency, the natural frequencies of the honeycomb sandwich plate with given crack length, crack direction and different locations in x- or y-directions are calculated, and the results are shown in Fig. 6(a) and (b). The results show that the natural frequencies rarely change with crack locations in the plate. This is because the given crack length is only 10% of plate length or width, and such a crack length is not large enough to be detected by structural natural frequencies.

Table 2
Natural frequencies of the cracked honeycomb sandwich plate (Hz)

Natural frequency order no.		1	2	3	4	5	6	7	8	9	10
Crack category	Crack length										
Intact	0	29.711	50.900	80.826	106.99	139.70	162.70	192.16	212.43	250.42	277.07
Longitudinal inner crack[a]	5% L	29.710	50.880	80.755	106.94	139.66	161.77	178.51	209.71	249.60	275.62
	10% L	29.712	50.841	80.800	106.24	139.71	158.37	174.31	210.44	250.76	274.57
	20% L	29.707	50.801	80.762	102.83	137.61	149.42	151.15	209.33	239.93	268.04
	30% L	29.865	50.784	80.867	90.507	111.40	139.31	140.62	196.72	220.48	267.51
Longitudinal edge crack[b]	5% L	29.710	50.883	80.827	106.97	139.66	162.12	190.47	211.19	249.76	277.72
	10% L	29.713	50.599	80.809	100.37	100.34	146.06	146.57	201.17	237.80	264.23
	20% L	29.716	49.682	72.518	80.868	93.41	145.67	146.55	202.32	239.64	263.81
	30% L	29.658	30.890	52.306	80.863	91.29	144.48	137.09	155.19	223.34	254.45
Transverse edge crack[b]	5% B	29.639	50.723	80.410	106.61	139.39	161.88	192.02	211.99	249.62	276.59
	10% B	29.373	50.000	79.123	104.99	138.02	159.93	191.88	209.17	245.24	275.32
	20% B	28.925	48.966	77.088	102.40	135.32	157.81	191.19	203.36	240.34	293.03
	30% B	25.703	30.526	50.499	75.054	90.73	136.88	147.79	192.67	225.89	250.68

[a] Inner crack – crack from plate edge.
[b] Edge crack – crack starting from plate edge.

As a summary, one can conclude that structural natural frequency is not suitable to detect crack damage less than 10% of the plate dimension, even up to 20% of the total size of a plate-like structure. Besides, it is very difficult to determine the location and severity of crack damage using natural frequencies.

In order to acquire the dynamic responses of a PVC honeycomb sandwich plate, two piezo-patches with a size of $25\times15\times0.28$ mm are bonded on the surface of the plate. One of them acts as an actuator and the other acts as a sensor. The experimental set-up for acquisition of the dynamic responses of the plate with different crack lengths is shown in Fig. 7. A square wave signal with 150 mV magnitude and 30 Hz frequency generated by the signal generator TGA 1230 is fed into the TRek Model 700 Piezo-driver. The 30 V voltage signal from the output of the piezo-driver is exerted on the piezo-patch actuator. Dynamic responses are measured using the piezo-patch sensor, and this signal is first fed into the B&K 2525 measuring amplifier, which can amplify the signal and filter out the noise using the 3–3 kHz band-pass function. Then, the output signal from the measuring amplifier is taken as the input of a computer with AD card for data sampling and storage.

In the experimental study, the plates are put on a soft sponge so that the free-free boundary conditions are simulated. Three honeycomb sandwich plates with different crack lengths of 3, 9 and 15 mm in longitudinal direction are studied, these crack lengths equal to 1%, 3%, and 5% of the plate length. Each dynamic response signal of these plates is decomposed into the 5th layer ($k = 5$) of wavelet transform, and

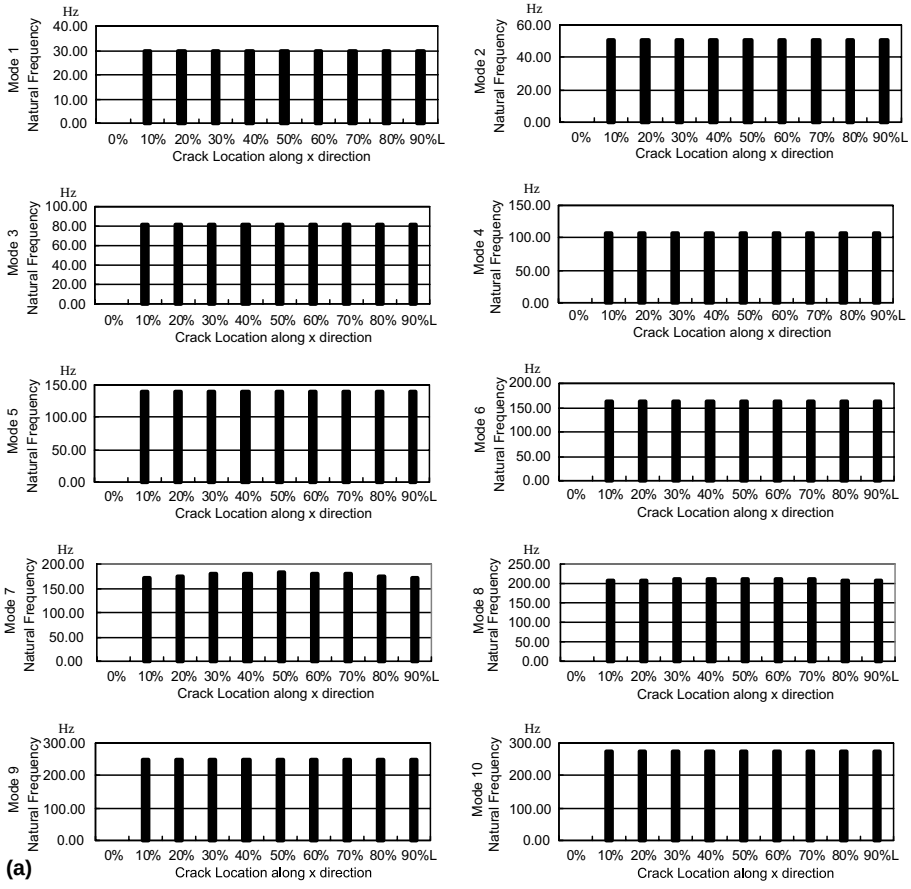

Fig. 6. Natural frequencies of a plate with different crack status.

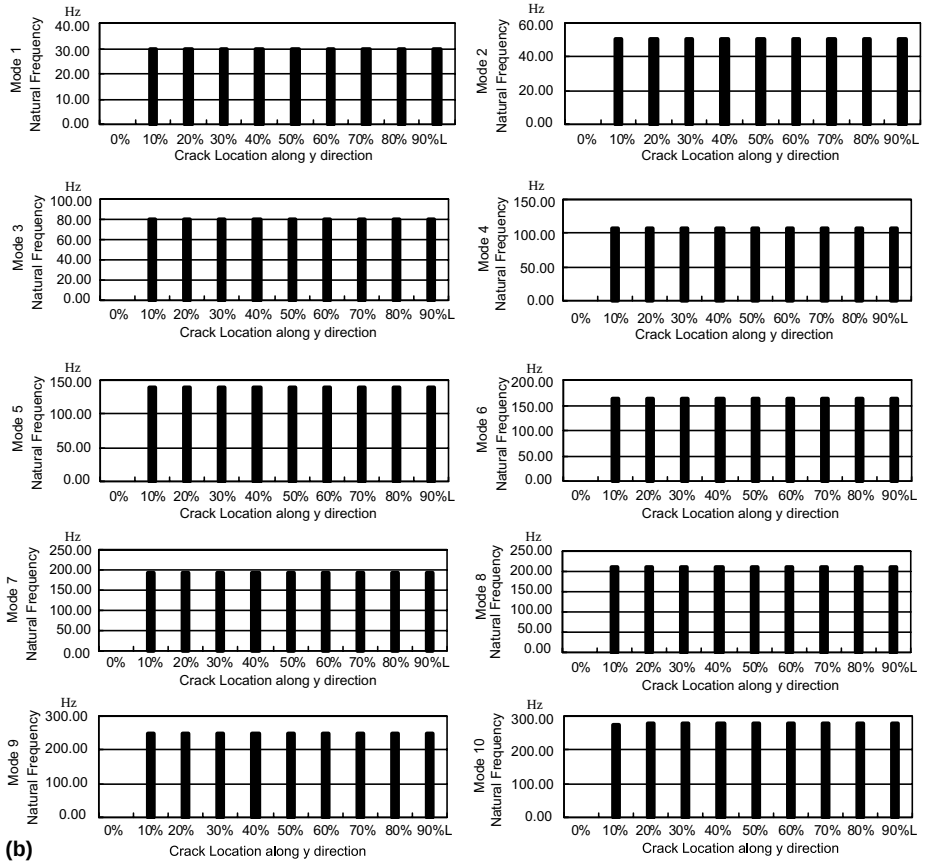

Fig. 6 (*continued*)

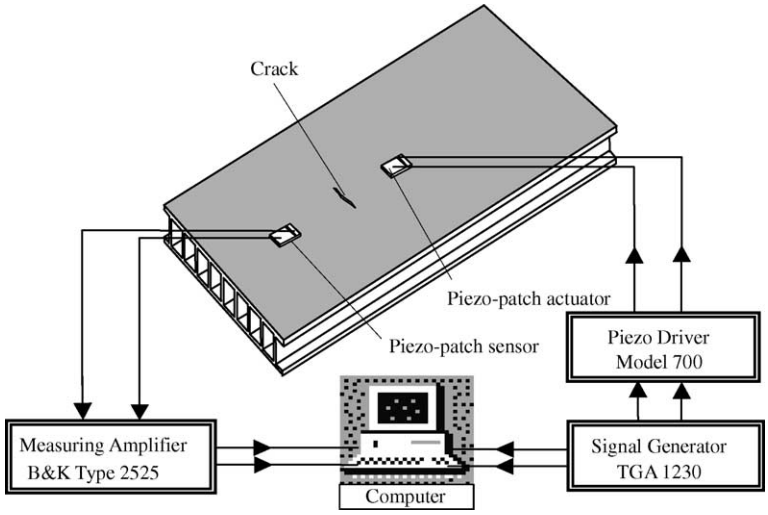

Fig. 7. Schematic diagram of experimental set-up for crack damage detection.

Table 3
Crack damage index V_d (%) of a honeycomb sandwich plate

Crack	3 mm (1% L)			9 mm (3% L)			15 mm (5% L)		
W.N	E	S	Error (%)	E	S	Error (%)	E	S	Error (%)
0	0.001	0.0009	8.48	0.069	0.0742	7.53	0.131	0.1403	7.07
1	−0.306	−0.329	7.55	2.129	2.3219	9.06	4.269	4.6567	9.08
2	−0.357	−0.380	6.58	0.465	0.5019	7.93	1.761	1.8941	7.56
3	1.687	1.9166	13.6	−12.59	−13.22	5.00	−28.48	−29.73	4.36
4	0.316	0.3496	10.6	4.619	5.0826	10.0	−1.060	−1.130	6.68
5	0.001	0.0009	9.19	−15.06	−15.72	4.37	−32.04	−33.18	3.55
6	1.985	2.2752	14.6	−9.385	−9.914	5.64	−24.98	−26.39	5.64
7	−0.541	−0.588	8.61	0.856	0.9273	8.32	3.930	4.2732	8.73
8	0.863	0.9657	11.8	2.899	3.1819	9.75	4.799	5.2526	9.45
9	1.240	1.4015	13.0	−17.16	−17.78	3.57	−16.68	−17.70	6.13
10	1.767	2.0161	14.0	−8.499	−9.022	6.16	−26.65	−28.00	5.09
11	0.001	0.0011	9.92	1.403	1.5259	8.75	3.245	3.5154	8.33
12	4.275	4.9169	15.0	−2.849	−3.052	7.15	7.815	8.6011	10.0
13	−1.509	−1.674	11.1	−4.966	−5.298	6.69	7.725	8.4745	9.70
14	0.472	0.5253	11.2	2.504	2.7392	9.39	2.140	2.3112	8.00
15	1.212	1.3633	12.4	−18.59	−19.07	2.57	−45.71	−46.89	2.59

W.N: wavelet number, E: experimental, S: numerical simulation.

16 wavelet sub-signals are obtained. The relative energy variations in these cases acquired using Eq. (33) are listed in Table 3.

According to the data in Table 3, some hints of crack damage detection can be found as follows: (1) When crack length is longer than 3% of the plate length, the largest element value of damage index vector will be larger than 10%, and errors between experimental and numerical results do not exceed 10%. (2) The larger the element value of the damage index vector, the smaller the errors between the experimental and numerical results. Especially, the errors of those larger element values (larger than 10%) are usually less than 5%. (3) When the crack length is shorter than 1% of the plate length, the element values of damage index vector are smaller, and the errors between the experimental and numerical results are generally larger than 10%. This indicates that these data are not reliable. The occurrence of so large errors for small crack may be due to random errors in experiment and modal truncation in numerical simulation, and the latter may be the main reason. This will be discussed in detail later.

Thus, one can conclude that if the largest element value of the damage index vector reaches 10%, some crack damage in a honeycomb sandwich plate can be detected using the method proposed in this paper. Describing complex damage status of a practical engineering structure requires a large amount of structural dynamic response data, which can be acquired by numerical simulation using an experimentally checked dynamic model.

In order to evaluate the ability of detecting crack extent using the method proposed in this paper, the damage index vector for crack length from 1% to 10% of the plate length are obtained using numerical simulation. The first three largest element values of each damage index vector are shown in Fig. 8. The results show that the largest element values of the damage index vector have an increasing tendency with the length of a crack, but the relation between them is not linear; if the largest element value reaching 10% is taken as an indicator of discovering structural crack, the smallest detectable crack extent using the damage index vector is about 2% of the structural length. Apparently, this method is more sensitive than using structural natural frequencies.

A special phenomenon discovered in this study is that structural damage information is often contained in some high order modes. Hence, the requirement for the established structural dynamic model for damage

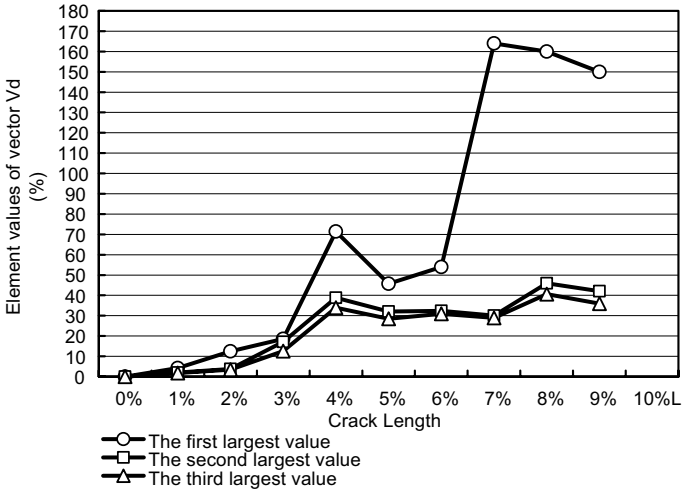

Fig. 8. The first three largest element values of damage index vector for different crack lengths.

detection is different from that for active structural vibration control, for which only several low order modes are usually considered. Structural damage detection requires more precise structural dynamic model, i.e. more modes should be included in the dynamic model. Otherwise, some small structural damage may be overlooked. Because only 20 modes are adopted in the dynamic model in this study, and the frequencies of these modes are very close, this may be a reason for the discrepancy between experimental and numerical results for small crack.

5. Conclusions

In this study, the ability of detecting crack damage in a honeycomb sandwich plate by using two types of structural vibration parameters (natural frequency and dynamic response) have been evaluated, and the feasibility of detecting small crack using method proposed in this study is also evaluated. We find that using structural natural frequency may not be suitable for detecting crack damage less than 10%, even up to 20% of the total size of a plate-like structure. Besides, it is very difficult to determine the location and category of crack damage with such a dimension. However, energy spectrum of wavelet transform signals of structural dynamic response has higher sensitivity to crack damage, it can exhibit structural damage status for a crack length close to 2% of the dimension of a plate-like structure. We also found that structural damage information is often contained in some high order modes of a structure, and more vibration modes should be included in structural dynamic model for detection of small damage.

Acknowledgements

The authors would like to thank for the support by Natural Science Foundation of China under the grant 50375123 and the Research Grants Council of Hong Kong Special Administrative Region of China under the project no. PolyU 5313/03E and the Research Committee of the Hong Kong Polytechnic University (project no. GT 621).

References

Chen, S.E., Venkatappa, S., Moody, J., Petro, S., GangaRao, H., 2000. A novel damage detection technique using scanning laser vibrometry and a strain energy distribution method. Materials Evaluation 58 (12), 1389–1394.

Chui, C.K., 1997. Wavelets: A Mathematical Tool for Signal Processing. Society for Industrial and Applied Mathematics, Philadelphia.

Collins, K.R., Plaut, R.H., Wauer, J., 1992. Free and forced longitudinal vibrations of a cantilevered bar with a crack. Journal of Vibration and Acoustics—Transactions of the ASME 114 (2), 171–177.

Doebling, S.W., Hemez, F.M., Peterson, L.D., Farhat, C., 1997. Improved damage location accuracy using strain energy-based mode selection criteria. AIAA Journal 35 (4), 693–699.

Farrar, C.R., Doebling, S.W., Nix, D.A., 2001. Vibration-based structural damage identification. Philosophical Transactions of the Royal Society of London Series A—Mathematical Physical And Engineering Sciences 359 (1778), 131–149.

Gobin, P.F., Jayet, Y., Baboux, J.C., et al., 2000. New trends in non-destructive evaluation in relation to the smart materials concept. International Journal of Systems Science 31 (11), 1351–1359.

Hou, Z., Noori, M., St Amand, R., 2000. Wavelet-based approach for structural damage detection. Journal of Engineering Mechanics—ASCE 126 (7), 677–683.

Hu, N., Wang, X., Fukunaga, H., Yao, Z.H., Zhang, H.X., Wu, Z.S., 2001. Damage assessment of structures using modal test data. International Journal of Solids and Structures 38 (18), 3111–3126.

Huebner, K.H., 2001. The Finite Element Method for Engineers. Wiley, New York.

Kosmatka, J.B., Ricles, J.M., 1999. Damage detection in structures by modal vibration characterization. Journal of Structural Engineering—ASCE 125 (12), 1384–1392.

Mallat, S.G., 1999. A Wavelet Tour of Signal Processing, 2nd ed. Academic Press, London, UK.

Nandwana, B.P., Maiti, S.K., 1997. Modeling of vibration of beam in presence of inclined edge or internal crack for its possible detection based on frequency measurements. Engineering Fracture Mechanics 58 (3), 193–205.

Ramamurti, V., Neogy, S., 1998. Effect of cracks on the natural frequency of cantilevered plates—a Rayleigh–Ritz solution. Mechanics of Structures and Machines 26 (2), 131–143.

Salawu, O.S., 1997. Detection of structural damage through changes in frequency: a review. Engineering Structures 19 (9), 718–723.

Strang, G., Nguyen, T., 1996. Wavelets and Filter Banks. Cambridge Press, Wellesley, MA.

Zhang, H., Schulz, M.J., Ferguson, F., Pai, P.F., 1999. Structural health monitoring using transmittance functions. Mechanical Systems and Signal Processing 13 (5), 765–787.

Zou, Y., Tong, L., Steven, G.P., 2000. Vibration-based model-dependent damage (delamination) identification and health monitoring for composite structures—a review. Journal of Sound and Vibration 230 (2), 357–378.